Ultrasonic material characterization by time-frequency analysis of backscattering noise

Vergara L., Fuente J. V., Gosálbez J., Miralles R., I. Bosch I.
Dpto. Comunicaciones, Univesidad Politécnica de Valencia
C/ Camino de Vera s/n
46022 Valencia, España,
Tel: 34963877308
 Fax, 349638777919
lvergara@dcom.upv.es

ABSTRACT

Ultrasonic backscattering noise appears in a large number of nondestructive testing applications, in the general area of tissue or material characterisation. We consider in this contribution the time-frequency analysis of backscattering noise with the aim of obtaining depth dependent profiles of some parameters related to the attenuation. The proposed analysis may have general applicability in the characterisation of materials or tissues having depth dependent properties. For example, it may be useful for measuring the penetration of repairing substances in deteriorated building elements. Also it may be of interest to obtain signatures of the material for classification purposes.

1. Introduction

When an ultrasonic pulse propagates inside a material suffers some variations related to the specimen properties. Of particular significance is the attenuation experimented by the pulse, which is, in general, frequency dependent. The attenuation will also be depth dependent if the material changes its properties with depth. It is most interesting to have a procedure for generating attenuation depth-frequency information for a complete characterisation of the material. This information may be derived from a time–frequency analysis [1] of the so-called backscattering noise [2], which corresponds to the superposition of the echoes backscattered by the material microstructure in a pulse-echo mode of inspection.

References [3]-[11] are some of the most interesting precedents of backscattering noise attenuation analysis. These precedents include not only material but also tissue oriented applications. In this paper we present some new contributions to the problem of attenuation estimation by means of time-frequency analysis of the backscattering noise. The first contribution is mainly theoretical; in general a rigorous analysis of the scattering composite effect in the time-frequency domain is difficult due to the variant nature of the underlying model. In the next section of this paper we present the depth-frequency function from which depth-frequency dependent attenuation is to be obtained.Then in section 3 we justify the use of time-frequency distributions as estimators of the depth-frequency function in a stochastic process context. This later leads us to practical methods for depth-frequency dependent attenuation estimation with two main novelties in comparison with the above mentioned previous works. First, attenuation estimation is not restricted to the case of linear dependence on frequency. Second, the scheme is suited for measuring depth variations of the attenuation, thus obtaining material depth profiles that could be used as material signatures for classification oriented

problems or to derive parameters to be correlated with material properties. They are also adequate to track inner variations in the properties of the material. Finally in Section 4, the proposed technique is applied to the characterisation of cement paste which is a basic element of mortar and concrete [14]. In particular, we have considered the extraction of parameters from the depth-frequency attenuation diagrams to be correlated with the cement paste porosity.

2. Depth-frequency function

We present in this section the depth-frequency function ($DFF(\mathbf{w}, z)$) and its relation with the depth-frequency dependent attenuation $\mathbf{a}_z(\mathbf{w})$. In the next section we will justify the use of time-frequency distributions ($TFD(t, \mathbf{w})$) as estimators of $DFF(\mathbf{w}, z)$. Let $p(t, z) = e(t, z)\exp\left(j\mathbf{w}_0 t\right)$ be the ultrasonic pulse that would be recorded at the transducer location from an isolated scatter located at depth z, where $\mathbf{w}_0$ is the ultrasonic pulse center frequency and $e(t, z)$ is the corresponding complex envelope of the pulse. Now let us consider that we were able to isolate a slice of material (figure 1) centred at depth z and having a width Δ small enough to avoid dispersion effects inside it, so the echoes from each scatter inside the slice would be the same except for a delay. Then, the ultrasonic backscattered signal would be the sum of all the contributions from all the scatters inside the slice

$$r(t, z) = \sum_{n=1}^{N(z)} A_n\, p(t - \mathbf{t}_n, z) = \sum_{n=1}^{N(z)} A_n\, e\left(t - \mathbf{t}_n, z\right)\exp\left(j\mathbf{w}_0\left(t - \mathbf{t}_n\right)\right) \tag{1}$$

where $N(z)$ is the number of scatters contributing inside the slice; $\{A_n\}$ are independent and identically distributed random variables (i.i.d.rr.vv.) representing, the reflectivity of each scattered echo and $\{\mathbf{t}_n\}$ are i.i.d.rr.vv. representing, the delay of each scattered echo. $\{A_n\}$ and $\{\mathbf{t}_n\}$ are also independent. Now let us consider the complex envelope of $r(t, z)$

$$r_c(t, z) = r(t, z)\exp\left(-j\mathbf{w}_0 t\right) = \sum_{n=1}^{N(z)} A_n\, e\left(t - \mathbf{t}_n, z\right)\exp\left(-j\mathbf{w}_0 \mathbf{t}_n\right) \tag{2}$$

If $E(\mathbf{w}, z)$ is the Fourier transform of $e(t, z)$ we can write the Fourier transform of (2) as

$$R_c(\mathbf{w}, z) = \sum_{n=1}^{N(z)} A_n\, E(\mathbf{w}, z)\exp\left(-j\left(\mathbf{w} + \mathbf{w}_0\right)\mathbf{t}_n\right) \tag{3}$$

It is generally accepted a exponential model for the attenuation

$$E(\mathbf{w}, z) = U(\mathbf{w})\exp\left(-\mathbf{a}_z(\mathbf{w})2z\right) \tag{4}$$

where $U(\mathbf{w}) = E_c(\mathbf{w}, 0)$ is the Fourier transform of the pulse sent into the material, much dependent on the ultrasonic system and the transducer used, and $\mathbf{a}_z(\mathbf{w})$ is the depth-frequency dependent attenuation. The factor 2 in the exponent accounts for the two-way travel in a pulse-echo inspection mode. From (4) and (3) we arrive to

$$R_c(\mathbf{w}, z) = U(\mathbf{w})\exp\left(-\mathbf{a}_z(\mathbf{w})4z\right)\sum_{n=1}^{N(z)} A_n\, \exp\left(-j\left(\mathbf{w} + \mathbf{w}_0\right)\mathbf{t}_n\right) \tag{5}$$

Now we are going to consider the expectation of the magnitude of (5) to deal with the random nature of the scatter location and reflectivity, the resulting function is what we call $DFF(\mathbf{w}, z)$

$$DFF(\mathbf{w}, z) = E\left[\left|R_c(\mathbf{w}, z)\right|^2\right] = \left|U(\mathbf{w})\right|^2 \exp\left(-\mathbf{a}_z(\mathbf{w})4z\right)E\left[\left|\sum_{n=1}^{N(z)} A_n\, \exp\left(-j\left(\mathbf{w} + \mathbf{w}_0\right)\mathbf{t}_n\right)\right|^2\right] \tag{6}$$

After some derivations we arrive to (7)

$$a_z(\boldsymbol{w}) = \frac{\log\left(|U(\boldsymbol{w})|^2\right) - \log(DFF(\boldsymbol{w},z)) + \log\left(N(z)\boldsymbol{s}_A^2 - N^2(z)E_A^2\right)}{4z} \qquad (7)$$

where $\boldsymbol{s}_A$ and E_A are respectively the standard deviation and the mean of the scatter reflectivity. Thus, in general, estimation of the depth-frequency dependent attenuation implies knowledge of $DFF(\boldsymbol{w},z)$, of the pulse magnitude $|U(\boldsymbol{w})|$, of the number of grains per unit volume (to estimate $N(z)$) and of the first and second moments of the scatter cross-section (that in general could be also z-dependent). However, if the material is homogenous we may consider $N(z) = N(0)$ for all z, then we can express the depth-frequency attenuation as

$$a_z(\boldsymbol{w}) = \frac{\log(DFF(\boldsymbol{w},0)) - \log(DFF(\boldsymbol{w},z))}{4z} \qquad (8)$$

where $DFF(\boldsymbol{w},0) = |U(\boldsymbol{w})|^2 \left(N\boldsymbol{s}_A^2 - N^2 E_A^2\right)$.

3. Estimating the depth-frequency function from time-frequency distributions.

Unfortunately, in practice we can not measure $DFF(\boldsymbol{w},z)$ directly, because we can not isolate slices, i.e., we can not directly measure the two dimensional signal $r_c(t,z)$. Instead we measure a one-dimensional signal (A-scan) $b(t)$ corresponding to the backscattering noise record in a given transducer location. Under which circumstances $b(t)$ and $r_c(t,z)$ may be related and how this can be done? Assuming that the ultrasonic pulse has finite time duration Δ_t and that the width Δ of the slices to define $DFF(\boldsymbol{w},z)$ is selected to be $\Delta = c\frac{\Delta_t}{2}$, where c is the ultrasonic speed of propagation, we have that

$$b(t) = r_c(t,z)\bigg|_{z=c\frac{t}{2}} \qquad (9)$$

That is, the assumed finite duration of the pulse make it possible to have a finite number of scatters contributing in a particular instant t to the waveform $b(t)$, and this finite number of scatters are inside an slice of width $\Delta = c\frac{\Delta_t}{2}$. At the end this allows relating $b(t)$ and $r_c(t,z)$. Note that the only hypothesis assumed in Section 2 about Δ was to be small enough to allow neglecting the dispersion effects inside the slice. Typical values for Δ_t and c, indicate that this hypothesis remains reasonable in practice (for example in the applications considered in Section 4, $\Delta = c\frac{\Delta_t}{2}$ is of the order of 0.1 mm). The equation (9), indicates that by recording backscattering noise we are moving into the *t-z* plane along a straight line that crosses the origin a has a slope $\frac{2}{c}$ (figure 2). The $TFD(\boldsymbol{w},t)$ is obtained by moving a finite time duration window along this straight line. Implicit on the many possible forms of computing $TFD(\boldsymbol{w},t)$ [1] is the (wide sense) stationarity inside the moving window interval. Let us consider a particular location of the moving window at $t = t_0$, $z = z_0 = c\frac{t_0}{2}$. We may extend the stationarity assumption to the shaded area of figure 2. For any *z* value inside this area we may consider that we have a truncated realisation of a *t*–dependent stationary stochastic process having a

power spectral density equal to $DFF(\boldsymbol{w}, z_0)$. If we could measure directly $r_c(t, z)$, the natural way for estimating $DFF(\boldsymbol{w}, z_0)$, would be to average estimates obtained by (local) spectral analysis over all the truncated realisations inside the shaded area. But, although moving along the diagonal of the shaded area, $b(t)$ is also a realisation of the same stationary stochastic process, so we can try to estimate $DFF(\boldsymbol{w}, z_0)$ by performing (local) spectral analysis on $b(t)$, that is

$$D\hat{F}F(\boldsymbol{w}, z_0) = TFD(\boldsymbol{w}, t)\Big|_{t = \frac{2}{c} z_0} \tag{10}$$

4. Application to the characterisation of cement paste

In this section we present the results of applying the attenuation analysis to measuring the degree of porosity of the cement paste. This is an important problem because cement paste is the main component of mortar and concrete [14]; the vulnerability (and so the durability) of these construction materials to external agents is much dependent on the cement porosity [15].
Porosity is dependent on water/cement ratio (w/c) and cement composition. On this study we choose two types of cement CEM II-AI 32.5 and 42.5. CEM 42.5 shows more resistance than CEM 32.5. Also, we consider two different w/c ratios, 0.4 and 0.5. Therefore, there are four cement paste types. We have built 6 probes, which are prisms of a size 16 x 4 x 4 (cm), for each type of cement paste. Three of the probes were used to measure in a destructive manner the porosity, following the method described in [16]. The other three probes were used to perform the ultrasonic nondestructive testing. In each probe we have recorded 20 records of backscattering noise along two sides of the prism. The ultrasonic equipment and the acquisition most significant data are:

-Ultrasonic pulse-receiver board: IPR-100, Physical Acoustics
-Transducer: Krautkramer KBA-10 MHz
-Digitalisation: Osciloscope Tektronix TDS-3012
-Sampling frequency: 125 MHz

We have computed the spectrogram of each record. The moving widow size was 300, and the overlapping lenght was 260, so we have one spectrum each 40 samples, thus corresponding to one spectrum each 0.6 mm (an average propagation velocity of 3500 m/s was considered to convert time scale into depth scale). Then we have averaged the 60 spectrograms corresponding to each type of cement paste, to have a smoothed $DFF(\boldsymbol{w}, z)$ estimate for each type of cement paste. The resulting four $DFF(\boldsymbol{w}, z)$ estimates are represented in figure 3 using a combined contour-grey scale plot: a contour plot where each contour is assigned a grey level value. h figure 4 we have consider the depth interval from 0.6 cm to 1.5 cm. Thus we can appreciate how the ultrasonic penetration is better for those cement pastes having lower water-cement ratio (0.4). For the 0.4 water-cement ratio we can also see the higher penetration for the cement paste having a more resistant cement (42.5). This effect is not so clear for the 0.5 water-cement ratio cases. Using equation (11) and the 60 averaged spectrograms, we have estimated $\boldsymbol{a}_z(\boldsymbol{w})$ for each type of cement paste. We have faced the possibility of extracting some parameter from the $\boldsymbol{a}_z(\boldsymbol{w})$ diagram to be correlated with the porosity of the cement paste. This has been done in two steps. First, from $\boldsymbol{a}_z(\boldsymbol{w})$, we have obtained a material signature (actually it could be used for classification) which is the mean attenuation in a selected band computed at each depth; we call it attenuation profile. In the figure 4 we show the profile of each type of cement paste, considering the band 11 MHz to 13 MHz and the depth interval 0.55 cm to 3.25 cm. Note the different attenuation levels exhibited by each type of cement paste. Also note the quasi-linear decaying trend showed by all the profiles after a given depth. This correspond to the 1/z effect of equation (11), which is predominant when the backscattering noise is very small with respect to the background noise, i.e., the numerator of equation (11) becomes constant with depth. Other frequency bands have been tested leading to similar results. From the profiles thus obtained we have extracted a

parameter, namely the profile area, to be correlated with the porosity estimates obtained by destructive methods. In figure 5 we represent the correlation curves.

Conclusions

We have considered in this paper the general problem of ultrasonic material characterisation by means of analysing the attenuation dependence on frequency and depth of backscattering noise. First we have shown (equation (10) and the simplified case of equation (11)) how the depth-frequency attenuation diagrams may be obtained from the depth-frequency function. Then, using stochastic process arguments, we have given a theoretical support to the use of time-frequency distributions as practical algorithms for deriving the depth-frequency function. Depth-frequency attenuation diagrams afford information that can be exploited in different ways. They may be used as observed diagnostic images in non-automatic procedures, but a more powerful benefit may be obtained by postprocessing the diagrams to derive material signatures. These signatures can be the input features to an automatic classifier if enough training is possible. We can also extract some relevant parameter from the signatures to be correlated with material properties. This later has been illustrated with a real problem: estimating the porosity of cement paste. To this end, we have proposed the use of signatures consisting in mean (in a given band) attenuation depth profiles. We have obtained good correlation properties between the profile area and the porosity. Other bands and parameters have been tested but results are not significantly different from those here presented**.**

References

[1] L. Cohen, Time-frequency distribution: a review, Prentice-Hall, NJ, 1995.
[2] L.Vergara, J.M. Páez, Backscattering gran noise modeling in ultrasonic non-destructive testing", Waves in Random Media 1 **(**1991) 81.
[3] J. Saniie J., N.M. Bilgutay, T.Wang, Signal Processing of Ultrasonic Backscattered Echoes for Evaluating the Microstructure of Materials, in Signal Processing and Pattern Recognition in Nondestructive Evaluation of Materials, Ed.Chen CH., Springer-Verlag Berlin, (1988) 87.
[4] P.He, J.F. Greenleaf,, Attenuation estimation on phantoms: stability test, Ultrason. Imaging 8, 1 (1986).
[5] H.S. Jang, T.K .Song, S.B. Park, Ultrasound attenuation estimation in soft tissue using the entropy difference of pulsed echoes between two adjacent envelope segments, Ultrason. Imaging 10 (1988) 248.
[6] J.A. Jensen, Estimation of pulses in ultrasound B-scan images, IEEE Trans. on Medical Imaging 10 (1991) 164.
[7] R. Kuc, R., Processing of diagnostic ultrasound signals, IEEE Acous. Speech ang Signal Process. Magazine, (1984) 19.
[8] R. Kuc., Estimating acoustic attenuation from reflected ultrasound signals: comparison of spectral-shift and spectral –difference approaches, IEEE Acous. Speech ang Signal Process. 32 (1984) 1.
[9] K.B. Rasmussen, Maximum likelihood estimation of the attenuated ultrasound pulse*,* IEEE Trans. on Signal Process. 42 (1994) 220.
[10] T. Baldeweck , A. Laugier, A. Herment, G. Berger, Application of autoregressive spectral analysis for ultrasound attenuation estimation: interest in highly attenuating medium, IEEE Trans. on Ultrason. Ferroelec. Freq. Contr. 42 (1995) 99.
[11] J.M. Girault JM, F. Ossant F., A. Ouahabi, D. Kouamé, F. Patat, Time-varying autoregressive spectral estimation for ultrasound attenuation in tissue characterisation, IEEE Trans. on Ultrason. Ferroelec. Freq. Contr., 45, (1998) 650.
[12] J. Saniie, T.Wang, N.M. Bilgutay, Analysis of homomorfic processing for ultrasonic grain signals, IEEE Trans. on Ultrason. Ferroelec. Freq. Contr., 36, (1989) 365.
[13] T.Wang, J. Saniie, Analysis of low-order autoregressive models for ultrasonic grain noise characterization, IEEE Trans. on Ultrason. Ferroelec. Freq. Contr. 38 (1991) 116.

[14] L.Vergara, R. Miralles, J.Gosálbez, F.J. Juanes, L.G.Ullate, J.J.Anaya, M.G. Hernández, M.A.G. Izquierdo, NDE ultrasonic methods to characterize the porosity of mortar, NDT&E International 34 (2001) 557.
[15] S.N. Alekseev, Durability of reinforced concrete in aggressive media, A.A. Balkema, Rotterdam, 1991.
[16] I. Janotka, Hydration of the cement paste with Na_2CO_3 addition, Ceramics, 45, (2001) 16.
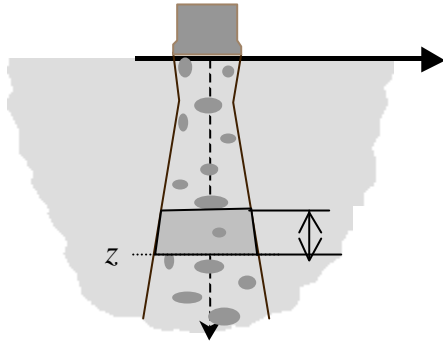
Figure 1. Isolated slice of material.
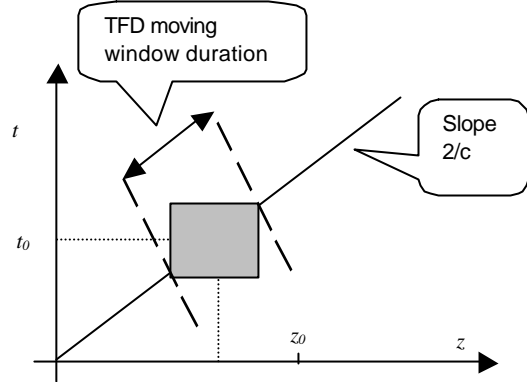
Figure 2 Explanation of the relationship between $r_c(t,z)$ and $b(t)$.
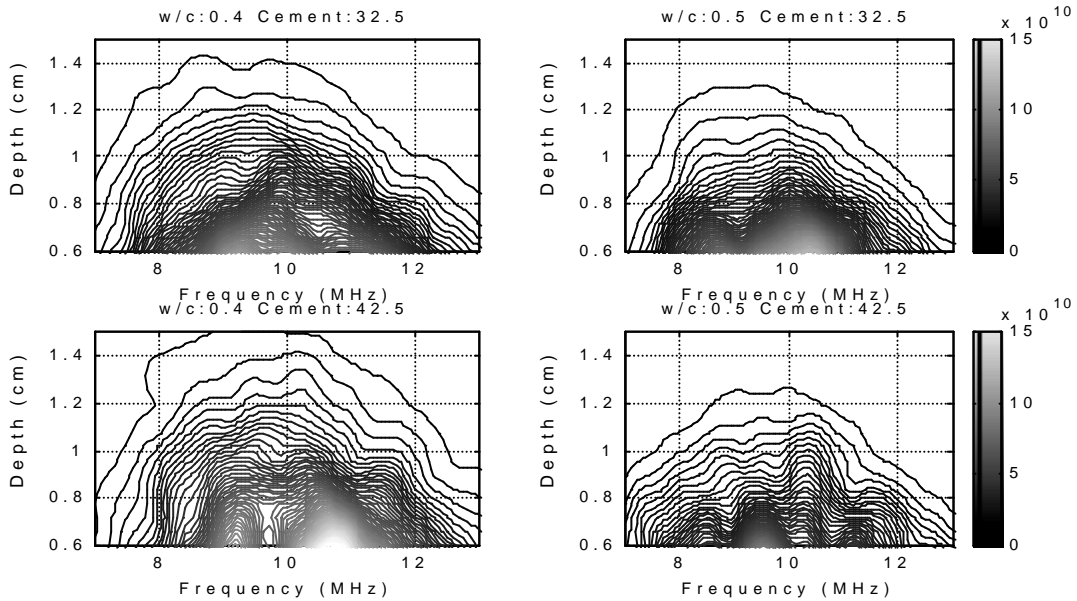
Figure 3. Averaged depth-frequency function for each type of cement paste.
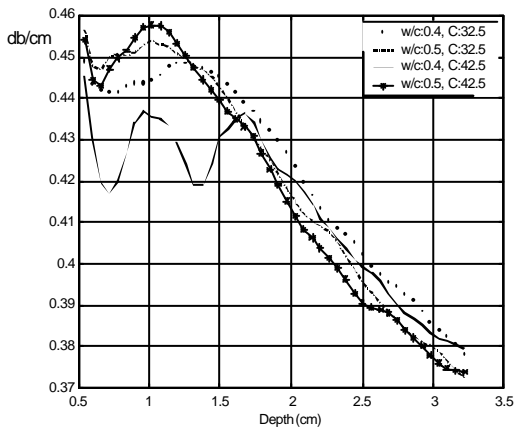
Figure 4. Material profile for each type of cement paste.
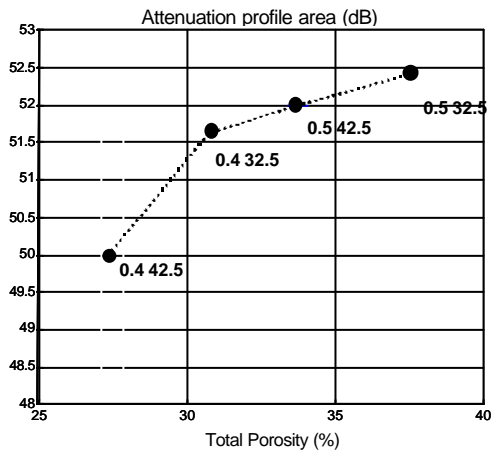
Figure 5. Parameter versus porosity for each type of cement paste.